IEEE Access
Multidisciplinary | Rapid Review | Open Access Journal

Received March 25, 2019, accepted April 17, 2019, date of publication April 23, 2019, date of current version May 3, 2019.

Digital Object Identifier 10.1109/ACCESS.2019.2912864

Bias Compensation for AOA-Geolocation of Known Altitude Target Using Single Satellite

CHAOXIN HE, MIN ZHANG, AND FUCHENG GUO

Sate Key Laboratory of Complex Electromagnetic Environment Effects on Electronics and Information System, National University of Defense Technology, Changsha 410073, China

Corresponding author: Min Zhang (zhangmin1984@126.com)

This work was supported in part by the National Defence Science and Technology Project Fund of China under Grant3101140, in part by the CASIC Aerospace Science and Technology Fund of China under Grant 179000203, and in part by the Shanghai Aerospace Science and Technology Innovation Fund of China under Grant SAST2015028.

ABSTRACT To reduce the passive localization bias caused by the nonlinearity between the target position and measurements under high noise level and poor geometry conditions, the bias compensation method for known altitude target geolocation using angles of arrival (AOA) obtained by a single satellite is proposed. The basic idea of this method is to estimate the bias first, and then subtract it from the estimation of the target position. Different from existing bias estimate methods which perform Taylor-series expansion on the maximum likelihood (ML) cost function, the proposed method directly applies Taylor-series expansion on the closed-form target location estimate. Interestingly, the expectations of the odd-order expansion terms of the Taylor-series in the proposed method are equal to zero, which indicates that higher bias estimation accuracy can be achieved with the same order of expansion compared with the existing methods. Furthermore, the theoretical analysis is performed and the result indicates that the Euclidean norm of the bias is independent of the azimuth angle and is positively correlated with the elevation angle. Finally, the computer simulations verify the superior performance of the proposed method and the theoretical analysis.

INDEX TERMS Angle of arrival, bias compensation, passive localization, satellite, Taylor-series expansion.

I. INTRODUCTION

Satellite-based passive localization technique has been extensively applied in many areas, such as radar, reconnaissance and wireless communications [1]–[7]. When the target is static, with known altitude on the surface of the Earth, its position can be uniquely determined using a single low orbit satellite geolocation system with two steps. First, the angle of arrival (AOA) of the target signal received at the single satellite is estimated [8], [9]. And then, the obtained AOA measurements are exploited to achieve target position using the closed-form or iterative-form estimator, such as the weighted least squares (WLS) [10], [11], or the maximum likelihood (ML) estimator [12] etc.

Because of the high nonlinearity between the AOA measurements and the target position, geolocation bias always exists in the target position estimate [13], [14]. When the noise is at a low level, the bias is not significant, and the mean square error (MSE) can be close to the Cramér-Rao lower bound (CRLB) [13]. However, the bias cannot be ignored when the noise is at a high level. The estimation performance may be seriously deteriorated [15], wherefore the MSE will deviate evidently from CRLB [16].

The direct way to reduce the geolocation bias caused by the nonlinearity is to progressively enhance the performance of geolocation algorithms. For example, the Weighted Stansfield in Three Dimensions (WS3D) algorithm [17] for bearings-only geolocation introduces a weighting matrix using the bearings variances and range information to reduce the estimation bias. However, it works well only at low or moderate noise level. The iterative Taylor-series method [18] using Gauss-Newton implementation of the maximum likelihood estimator (MLE) is asymptotically unbiased. But this iterative-form method generally needs an initial position guess that is near the actual solution, otherwise it may converge to a local minimum solution.

Another alternative is to first obtain the bias and then subtract it from the target position estimation. Reference [19] proposed a bias compensation algorithm from the weighted least squares (WLS) estimator in multipulse time difference

The associate editor coordinating the review of this manuscript and approving it for publication was Qiang Yang.

of arrival (TDOA) localization. Reference [20] developed a reduced-bias pseudolinear estimator for bias compensation in bearings-only geolocation. These closed-form bias are derived by calculating the expectation of weighted noise under the assumption that the number of measurements is enough large. However, this assumption may not be available in most cases. Gavish and Weiss [21] derived the theoretical bias of the MLE for bearings-only tracking. They found that in contrast with the closed-form estimator, the MLE provided asymptotic unbiased estimates. Rui and Ho [15], [22] derived the bias by performing Taylor-series expansion of the maximum likelihood (ML) cost function up to second order. This method can achieve a good result at small or moderate noise level with good geolocation geometry. However, the performance of the bias estimation will be deteriorated when geometry is poor and the noise level is high.

To solve this problem in the bias estimator using Taylor-series expansion, one obvious idea is to expand the Taylor-series in [22] up to three and even higher order, but it is intractable to derive and computational intensively. Motivated by these facts, a new closed-form bias estimate and compensate algorithm is proposed in this paper. Bias compensation is done by first estimating the bias and then subtracting it from the target position estimate. The major contributions and innovations of this paper can be concluded as follows.

- A closed-form target position estimate is first obtained using the elevation and azimuth angles by a single satellite under the spherical Earth model. The proposed bias estimator is then derived by Taylor-series expansion on the closed-form target location estimate, instead of the ML cost function [22].
- It is observed that the expectations of the odd-order Taylor-series expansion terms in the proposed bias estimate method are equal to zero. This means that all bias information is contained in the even-order expansions. Thus, the same expansion order can be used to achieve higher bias estimation accuracy compared with existing methods.
- The closed-form formula of the Euclidean norm of the estimated bias is derived. Theoretical analysis indicates that the Euclidean norm of the bias is positively correlated with the elevation angle and the measurement noise level, but independent of the azimuth angle.

The rest of this paper is organized as follows. We formulate the geolocation problem in consideration in Section II. The proposed bias estimation and compensation method is derived in Section III. Bias estimate analysis is presented in Section IV. Simulation results and conclusions are given in Section V and Section VI respectively.

II. PROBLEM FORMULATION

The geolocation scenario by a single satellite is shown in Fig. 1. There is a static emitter on the surface of the Earth with known altitude h_0. The position of the emitter and satellite under the ECEF (earth-center earth-fixed) coordinates [23] are denoted as $\boldsymbol{x}_T^0 = \begin{bmatrix} x_T^0 & y_T^0 & z_T^0 \end{bmatrix}^{\mathrm{T}}$ and $\boldsymbol{x}_s^0 = \begin{bmatrix} x_s^0 & y_s^0 & z_s^0 \end{bmatrix}^{\mathrm{T}}$.

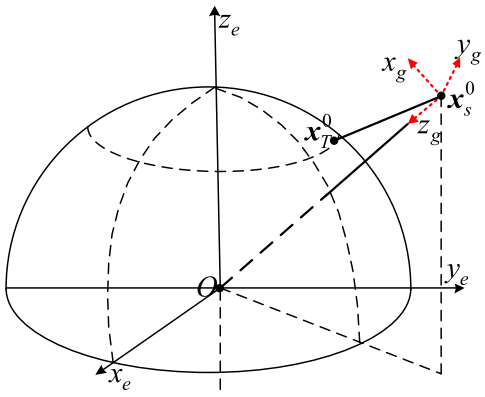

FIGURE 1. Geolocation scenario by a single satellite (x_e, y_e, and z_e are the coordinate axes of the earth-center earth-fixed coordinate system. x_g, y_g, and z_g are the coordinate axes of the satellite coordinate system).

The satellite coordinate system [2], denoted as System $\boldsymbol{g}$, is defined as follows. The origin of the coordinates lies in the center of the satellite, the x_g axis is the longitudinal axis of the satellite, with the forward direction of the satellite motion; the y_g axis lies in the starboard of the satellite, perpendicular to the longitudinal axis; and the z_g axis is downwards of the coordinate system, points to the earth center.

Without the loss of generality, we consider the geolocation problem under the spherical Earth model. The unknown target position $\boldsymbol{x}_T^0$ is assumed to be related to the target altitude via [24]

$$\boldsymbol{x}_T^{0\mathrm{T}} \boldsymbol{x}_T^0 = (R + h_0)^2, \tag{1}$$

where $R = 6378.137$ km is the equatorial radius of the earth, h_0 is the altitude of the target.

The sensors mounted on the satellite receive the source signal and then estimate the elevation angle and azimuth angle. Let α^0 and β^0 be the true elevation angle and azimuth angle in the satellite coordinate system [23]. The estimated elevation angle α and azimuth angle β can be expressed as,

$$\boldsymbol{m} = \begin{bmatrix} \alpha & \beta \end{bmatrix}^{\mathrm{T}} = \boldsymbol{m}^0 + \boldsymbol{\varepsilon}_m, \tag{2}$$

where $\boldsymbol{m}^0 = \begin{bmatrix} \alpha^0 & \beta^0 \end{bmatrix}^{\mathrm{T}}$ and $\boldsymbol{\varepsilon}_m = \begin{bmatrix} \varepsilon_\alpha & \varepsilon_\beta \end{bmatrix}^{\mathrm{T}}$ is the additive measurement noise. We assume that $\boldsymbol{\varepsilon}_m$ is Gaussian noise with zero mean and covariance matrix $\boldsymbol{Q}$. Thus, the probability density function of measurement vector $\boldsymbol{m}$ is

$$p(\boldsymbol{m}) = \frac{1}{\sqrt{|2\pi \boldsymbol{Q}|}} \exp\left(-\frac{1}{2} \left(\boldsymbol{m} - \boldsymbol{m}^0 \right)^{\mathrm{T}} \boldsymbol{Q}^{-1} \left(\boldsymbol{m} - \boldsymbol{m}^0 \right) \right), \tag{3}$$

where $\boldsymbol{Q} = \begin{bmatrix} \sigma_1^2 & 0 \\ 0 & \sigma_2^2 \end{bmatrix}$, σ_1 and σ_2 are the noise intensity of observed elevation and azimuth angles respectively.

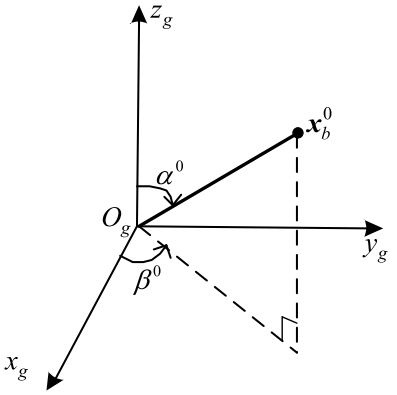

FIGURE 2. Definitions of the elevation angle and azimuth angle in the satellite coordinate system (x_b^0 is the line of sight vector).

As shown in Fig. 2, definitions of α^0 and β^0 are given as,

$$\alpha^0 = \arccos\left(\frac{z_b^0}{\sqrt{\left(x_b^0\right)^2+\left(y_b^0\right)^2+\left(z_b^0\right)^2}}\right), \tag{4a}$$

$$\beta^0 = \arctan\left(\frac{y_b^0}{x_b^0}\right), \tag{4b}$$

where $\boldsymbol{x}_b^0 = \begin{bmatrix} x_b^0 & y_b^0 & z_b^0 \end{bmatrix}$ is the line of sight (LOS) [2] vector in the satellite coordinate system (System $\boldsymbol{g}$), and it can be calculated by

$$\boldsymbol{x}_b^0 = \boldsymbol{M}\left(\boldsymbol{x}_s^0 - \boldsymbol{x}_T^0\right), \tag{5}$$

where $\boldsymbol{M}$ is a coordinate transformation matrix [23] for converting the coordinates from the ECEF coordinate system to the satellite coordinate system. It can be calculated by some matrix operations when the satellite attitude angles (yaw, pitch, and roll) are measured [23]. Denoting the yaw, pitch, and roll of the satellite as ϵ, ε, and ζ respectively, then $\boldsymbol{M}$ can be calculated by,

$$\boldsymbol{M} = \boldsymbol{P}_x(\zeta)\boldsymbol{P}_y(\varepsilon)\boldsymbol{P}_z(\epsilon), \tag{6}$$

where $\boldsymbol{P}_x(\zeta)$, $\boldsymbol{P}_y(\varepsilon)$, and $\boldsymbol{P}_z(\epsilon)$ are rotation functions,

$$\boldsymbol{P}_x(\zeta) = \begin{bmatrix} 1 & 0 & 0 \\ 0 & \cos(\zeta) & \sin(\zeta) \\ 0 & -\sin(\zeta) & \cos(\zeta) \end{bmatrix}, \tag{7}$$

$$\boldsymbol{P}_y(\varepsilon = \begin{bmatrix} \cos(\varepsilon) & 0 & -\sin(\varepsilon) \\ 0 & 1 & 0 \\ \sin(\varepsilon) & 0 & \cos(\varepsilon) \end{bmatrix}, \tag{8}$$

$$\boldsymbol{P}_z(\epsilon = \begin{bmatrix} \cos(\epsilon) & \sin(\epsilon) & 0 \\ -\sin(\epsilon) & \cos(\epsilon) & 0 \\ 0 & 0 & 1 \end{bmatrix}. \tag{9}$$

Thus, we can deduce that the determinant of $\boldsymbol{M}$ is equal to 1,

$$|\boldsymbol{M}| = |\boldsymbol{P}_x(\zeta)||\boldsymbol{P}_y(\varepsilon)||\boldsymbol{P}_z(\epsilon)| = 1. \tag{10}$$

where $|*|$ denotes the determinant of a matrix.

The problem at hand now is to use the measurement given in (2) to determine the target position and compensate the geolocation bias.

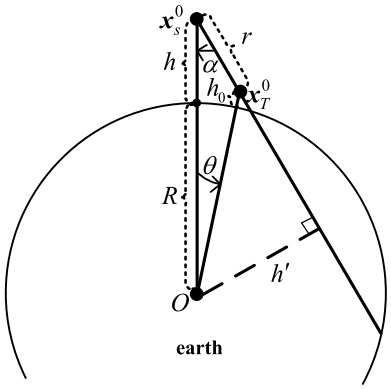

FIGURE 3. Distance between the target and satellite, and its relationship with the angle measurement.

III. BIAS COMPENSATION

In this section, a closed-form target location estimator using elevation and azimuth angle is firstly derived. And then, the bias estimator is proposed by applying Taylor-series expansion on the derived target location estimate. Meanwhile, theoretical analysis is performed to manifest the characteristic of the proposed method. Finally, bias is compensated by subtracting the estimated bias from the target location estimate.

A. CLOSED FORM LOCALIZATION ESTIMATOR

The target location estimate can be obtained from (5) that

$$\hat{\boldsymbol{x}}_T = \boldsymbol{x}_s^0 - \boldsymbol{M}^{-1}\hat{\boldsymbol{x}}_b, \tag{11}$$

where $\hat{\boldsymbol{x}}_b$ is the measured LOS vector in the satellite coordinate system.

By the definition of elevation angle α and azimuth angle β, $\hat{\boldsymbol{x}}_b$ can be written as [2]

$$\begin{aligned}\hat{\boldsymbol{x}}_b &= r\boldsymbol{u} = \begin{bmatrix} \hat{x}_b & \hat{y}_b & \hat{z}_b \end{bmatrix}^{\mathrm{T}} \\ &= \begin{bmatrix} r\sin\alpha\cos\beta & r\sin\alpha\sin\beta & -r\cos\alpha \end{bmatrix}^{\mathrm{T}}, \end{aligned} \tag{12}$$

where $\boldsymbol{u} = \begin{bmatrix} \sin\alpha\cos\beta & \sin\alpha\sin\beta & -\cos\alpha \end{bmatrix}^{\mathrm{T}}$, r is the distance between the target and satellite. It can be seen from (11) and (12) that once r is obtained, the target location $\hat{\boldsymbol{x}}_T$ can be easily estimated.

According to the geometry configuration shown in Fig. 3, we can obtain that

$$\begin{aligned} r = \left\|\boldsymbol{x}_T^0 - \boldsymbol{x}_s^0\right\| &= (R+h)\cos\alpha \\ &\quad - (R+h_0)\cos(\alpha+\theta), \end{aligned} \tag{13}$$

$$h' = (R+h)\sin\alpha, \tag{14a}$$

$$\sin(\alpha+\theta) = \frac{h'}{(R+h_0)}. \tag{14b}$$

where $\|*\|$ denotes the Euclidean norm, h is the satellite altitude, θ is the geocentric angle between the satellite and the target.

Therefore, the cosine of angle $\alpha+\theta$ is

$$\cos(\alpha+\theta) = \cos\left(\arcsin\left(\frac{h'}{(R+h_0)}\right)\right)$$

$$= \sqrt{1 - \frac{(R+h)^2 \sin^2 \alpha}{(R+h_0)^2}}. \quad (15)$$

After Substituting (15) into (14a), the calculation of parameter r can be given by

$$r = (R+h)\cos\alpha - (R+h_0)\sqrt{1 - \frac{(R+h)^2 \sin^2 \alpha}{(R+h_0)^2}}. \quad (16)$$

It is observed that r is related to R, h, h_0, and α. Therein the radius of the earth R is a constant, the altitude of target h_0 and satellite h are known variables. Thus, the distance between the satellite and target r only depends on the elevation angle α, and is independent of the azimuth angle β.

Finally, we can obtain the closed-form target location estimate $\hat{\boldsymbol{x}}_T$ from (11),(12) and (16),

$$\hat{\boldsymbol{x}}_T = \boldsymbol{x}_s^0 - \boldsymbol{M}^{-1} \begin{bmatrix} r\sin\alpha\cos\beta \\ r\sin\alpha\sin\beta \\ -r\cos\alpha \end{bmatrix}. \quad (17)$$

B. BIAS ESTIMATION AND COMPENSATION

In this subsection, we first derive the closed-form bias formula. Bias is then deducted from the target location estimate.

The geolocation bias is defined as [13]

$$\boldsymbol{b}_{\hat{\boldsymbol{x}}_T} = E\left(\hat{\boldsymbol{x}}_T - \boldsymbol{x}_T^0\right), \quad (18)$$

where $E(*)$ represent the statistical expectation .

Substituting (11) into (18) gives

$$\boldsymbol{b}_{\hat{\boldsymbol{x}}_T} = \hat{\boldsymbol{M}}^{-1} E\left(\hat{\boldsymbol{x}}_b - \boldsymbol{x}_b^0\right). \quad (19)$$

Equation (19) shows that the estimation of $\boldsymbol{b}_{\hat{\boldsymbol{x}}_T}$ can be replaced by deriving $E\left(\hat{\boldsymbol{x}}_b - \boldsymbol{x}_b^0\right)$. Let

$$\boldsymbol{b}_{\hat{\boldsymbol{x}}_b} = E\left(\hat{\boldsymbol{x}}_b - \boldsymbol{x}_b^0\right). \quad (20)$$

It can be indicated from (12) that $\hat{\boldsymbol{x}}_b$ is a nonlinear function of the measurement vector $\boldsymbol{m}$. The Taylor-series expansion of $\hat{\boldsymbol{x}}_b$ at $\boldsymbol{m}^0 = \begin{bmatrix} \alpha^0 & \beta^0 \end{bmatrix}^{\mathrm{T}}$ up to the nth order is

$$\begin{aligned} \hat{\boldsymbol{x}}_b = \boldsymbol{x}_b^0 &+ \left.\frac{\partial \hat{\boldsymbol{x}}_b}{\partial \boldsymbol{m}^{\mathrm{T}}}\right|_{\boldsymbol{m}=\boldsymbol{m}^0} \left(\boldsymbol{m} - \boldsymbol{m}^0\right) \\ &+ \frac{1}{2} \begin{bmatrix} \left(\boldsymbol{m} - \boldsymbol{m}^0\right)^{\mathrm{T}} \left.\frac{\partial^2 \hat{x}_b}{\partial \boldsymbol{m} \partial \boldsymbol{m}^{\mathrm{T}}}\right|_{\boldsymbol{m}=\boldsymbol{m}^0} \left(\boldsymbol{m} - \boldsymbol{m}^0\right) \\ \left(\boldsymbol{m} - \boldsymbol{m}^0\right)^{\mathrm{T}} \left.\frac{\partial^2 \hat{y}_b}{\partial \boldsymbol{m} \partial \boldsymbol{m}^{\mathrm{T}}}\right|_{\boldsymbol{m}=\boldsymbol{m}^0} \left(\boldsymbol{m} - \boldsymbol{m}^0\right) \\ \left(\boldsymbol{m} - \boldsymbol{m}^0\right)^{\mathrm{T}} \left.\frac{\partial^2 \hat{z}_b}{\partial \boldsymbol{m} \partial \boldsymbol{m}^{\mathrm{T}}}\right|_{\boldsymbol{m}=\boldsymbol{m}^0} \left(\boldsymbol{m} - \boldsymbol{m}^0\right) \end{bmatrix} \\ &+ \ldots + \boldsymbol{b}^n\left(\boldsymbol{m}^0\right). \end{aligned} \quad (21)$$

where $\boldsymbol{b}^n\left(\boldsymbol{m}^0\right)$ is the nth order expansion term of $\hat{\boldsymbol{x}}_b$,

$$\boldsymbol{b}^n\left(\boldsymbol{m}^0\right) = \left[b_x^n\left(\boldsymbol{m}^0\right)\ b_y^n\left(\boldsymbol{m}^0\right)\ b_z^n\left(\boldsymbol{m}^0\right) \right]^{\mathrm{T}}, \quad (22)$$

with

$$f_n(p) = \left(\alpha - \alpha^0\right)^p \left(\beta - \beta^0\right)^{n-p}, \quad (23a)$$

$$b_x^n\left(\boldsymbol{m}^0\right) = \frac{1}{n!} \sum_{p=0}^{n} f_n(p) C_n^p \left.\frac{\partial^n \hat{x}_b}{\partial \alpha^p \partial \beta^{n-p}}\right|_{\boldsymbol{m}=\boldsymbol{m}^0}, \quad (23b)$$

$$b_y^n\left(\boldsymbol{m}^0\right) = \frac{1}{n!} \sum_{p=0}^{n} f_n(p) C_n^p \left.\frac{\partial^n \hat{y}_b}{\partial \alpha^p \partial \beta^{n-p}}\right|_{\boldsymbol{m}=\boldsymbol{m}^0}, \quad (23c)$$

$$b_z^n\left(\boldsymbol{m}^0\right) = \frac{1}{n!} \sum_{p=0}^{n} f_n(p) C_n^p \left.\frac{\partial^n \hat{z}_b}{\partial \alpha^p \partial \beta^{n-p}}\right|_{\boldsymbol{m}=\boldsymbol{m}^0}. \quad (23d)$$

Under the independent Gaussian noise assumption we get that [25],

$$E\left(f_n(p)\right) = 0, \quad \text{if } n = \text{odd}. \quad (24)$$

Substituting (24) into (22) gives

$$E\left(\boldsymbol{b}^n\left(\boldsymbol{m}^0\right)\right) = \boldsymbol{0}, \quad \text{if } n = \text{odd}. \quad (25)$$

Using the above conclusion and ignoring the expansion terms higher than second order yields

$$\boldsymbol{b}_{\hat{\boldsymbol{x}}_b} = E\left(\boldsymbol{b}^2\left(\boldsymbol{m}^0\right)\right) = \left[b_x \quad b_y \quad b_z \right]^{\mathrm{T}}, \quad (26)$$

where

$$b_x = E\left(b_x^2\left(\boldsymbol{m}^0\right)\right) = \left.\left(\frac{\partial^2 \hat{x}_b}{\partial \alpha^2}\sigma_1^2 + \frac{\partial^2 \hat{x}_b}{\partial \beta^2}\sigma_2^2\right)\right|_{\boldsymbol{m}=\boldsymbol{m}^0} \quad (27)$$

$$b_y = E\left(b_y^2\left(\boldsymbol{m}^0\right)\right) = \left.\left(\frac{\partial^2 \hat{y}_b}{\partial \alpha^2}\sigma_1^2 + \frac{\partial^2 \hat{y}_b}{\partial \beta^2}\sigma_2^2\right)\right|_{\boldsymbol{m}=\boldsymbol{m}^0} \quad (28)$$

$$b_z = E\left(b_z^2\left(\boldsymbol{m}^0\right)\right) = \left.\left(\frac{\partial^2 \hat{z}_b}{\partial \alpha^2}\sigma_1^2 + \frac{\partial^2 \hat{z}_b}{\partial \beta^2}\sigma_2^2\right)\right|_{\boldsymbol{m}=\boldsymbol{m}^0} \quad (29)$$

Thus, we can present the desired bias in the ECEF coordinates

$$\boldsymbol{b}_{\hat{\boldsymbol{x}}_T} = \boldsymbol{M}^{-1} \boldsymbol{b}_{\hat{\boldsymbol{x}}_b}. \quad (30)$$

The estimated bias can be used to improve the localization accuracy through bias compensation, which is done by subtracting the estimated bias from the target location estimation [20]. A bias compensated target location estimate can be formulated as

$$\hat{\boldsymbol{x}}_{T_{BC}} = \hat{\boldsymbol{x}}_T - \boldsymbol{b}_{\hat{\boldsymbol{x}}_T}. \quad (31)$$

If we have multiple location estimates of a static target, the bias compensated target location estimate can be then calculated by using the weighted least squares (WLS) estimator [13],

$$\hat{\boldsymbol{x}}_{W_{BC}} = \left(\sum_{k=1}^{K} \boldsymbol{R}_k^{-1}\right)^{-1} \sum_{k=1}^{K} \boldsymbol{R}_k^{-1} \hat{\boldsymbol{x}}_{T_{BC}}(k), \quad (32)$$

where K is the observation times for a given target. $\hat{\boldsymbol{x}}_{T_{BC}}(k)$ is the kth bias compensated target location estimate. $\boldsymbol{R}_k$ is the weighting matrix, which is the CRLB of the geolocation error.

It can be seen from (31) that the key to bias compensation is the bias estimation. The accuracy of the bias estimation determines the performance of bias compensation. The proposed bias estimate method has the property that the expectations of the odd-order expansion terms are equal to zero. This means that all bias information is contained

in the even-order expansions. Thus, we can achieve higher bias estimation accuracy with the same order of expansion compared to existing methods. Furthermore, we can obtain better geolocation performance after bias compensation.

IV. BIAS ESTIMATE ANALYSIS

To find the mathematical relationship between the bias estimate and the elevation, azimuth angle, and noise intensity, we derive the Euclidean norm of the bias in this section.

The Euclidean norm of the bias can be derived from (30). By noting that $|\boldsymbol{M}| = 1$ has been derived in (10), we get that

$$\left\|\boldsymbol{b}_{\hat{\boldsymbol{x}}_T}\right\| = \left\|\boldsymbol{M}^{-1}\boldsymbol{b}_{\hat{\boldsymbol{x}}_b}\right\| = \left\|\boldsymbol{b}_{\hat{\boldsymbol{x}}_b}\right\|. \tag{33}$$

Without the loss of generality, the noise variances of the azimuth and elevation angle measurements are normally the same, which means that $\sigma_1^2 = \sigma_2^2 = \sigma^2$. Substituting the definition of $\boldsymbol{b}_{\hat{\boldsymbol{x}}_b}$ (26) into $\left\|\boldsymbol{b}_{\hat{\boldsymbol{x}}_b}\right\|$ yields

$$\left\|\boldsymbol{b}_{\hat{\boldsymbol{x}}_b}\right\| = \frac{\sigma^2}{2}\sqrt{\begin{array}{c}\left(\frac{\partial^2\hat{x}_b}{\partial\alpha^2}+\frac{\partial^2\hat{x}_b}{\partial\beta^2}\right)^2+\left(\frac{\partial^2\hat{y}_b}{\partial\alpha^2}+\frac{\partial^2\hat{y}_b}{\partial\beta^2}\right)^2 \\ +\left(\frac{\partial^2\hat{z}_b}{\partial\alpha^2}+\frac{\partial^2\hat{z}_b}{\partial\beta^2}\right)^2\end{array}}. \tag{34}$$

Substituting the definition of $\hat{\boldsymbol{x}}_b$ (12) into (34) yields

$$\frac{\partial^2\hat{x}_b}{\partial\beta^2} = -\sin\alpha\cos\beta\triangle_1, \tag{35a}$$

$$\frac{\partial^2\hat{y}_b}{\partial\beta^2} = -\sin\alpha\sin\beta\triangle_1, \tag{35b}$$

$$\frac{\partial^2\hat{z}_b}{\partial\beta^2} = 0. \tag{35c}$$

$$\frac{\partial^2\hat{x}_b}{\partial\alpha^2} = -\sin\alpha\cos\beta\triangle_2, \tag{36a}$$

$$\frac{\partial^2\hat{y}_b}{\partial\alpha^2} = -\sin\alpha\sin\beta\triangle_2, \tag{36b}$$

$$\frac{\partial^2\hat{z}_b}{\partial\alpha^2} = -\frac{\partial^2\left(r\cos\alpha\right)}{\partial\alpha^2} = \triangle_3. \tag{36c}$$

where

$$\triangle_1 = (R+h_0)\sqrt{1-\frac{(R+h)^2\sin^2\alpha}{R^2}} - (R+h)\cos\alpha, \tag{37}$$

$$\triangle_2 = \frac{k_2}{R^3k_1}, \tag{38a}$$

$$k_1 = \left(1-\frac{(R+h)^2\sin^2\alpha}{R^2}\right)^{\frac{3}{2}}, \tag{38b}$$

$$k_2 = \boldsymbol{v}_1^{\mathrm{T}}\boldsymbol{A}\boldsymbol{v}_2. \tag{38c}$$

where

$$\boldsymbol{v}_1 = \left[\cos^4\alpha \quad \cos^2\alpha \quad \cos\alpha \quad 1\right], \tag{39}$$

$$\boldsymbol{v}_2 = \left[R^4 \quad R^3h \quad R^2h^2 \quad Rh^3 \quad h^4\right], \tag{40}$$

$$\boldsymbol{A} = \begin{bmatrix} 4 & 16 & 24 & 16 & 4 \\ 0 & -12 & -30 & -24 & -6 \\ 0 & -4k_1 & 0 & 0 & 0 \\ -4k_1 & 2 & 9 & 8 & 2 \end{bmatrix}, \tag{41}$$

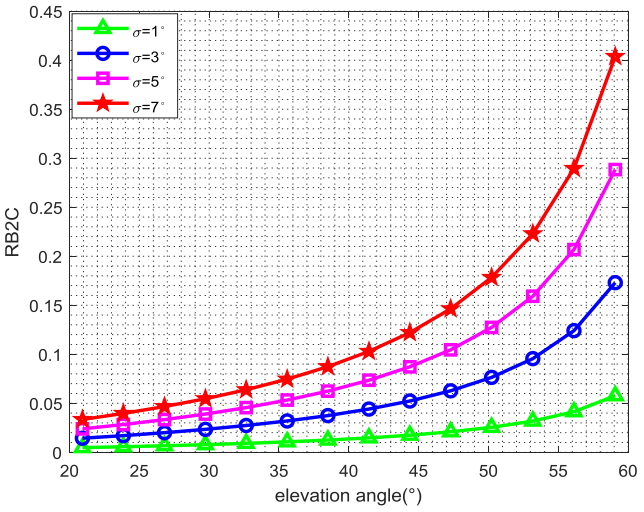

FIGURE 4. RB2C results versus elevation angle.

Substituting (36a) and (36) into (34) gives

$$\left\|\boldsymbol{b}_{\hat{\boldsymbol{x}}_T}\right\| = \frac{\sigma^2}{2}\sqrt{\sin^2\alpha\left(\triangle_1+\triangle_2\right)+\triangle_3}, \tag{42}$$

where $\triangle_1$, $\triangle_2$, and $\triangle_3$ are independent of the azimuth angle β.

It can be obviously seen from (42) that the Euclidean norm of the bias is independent of the azimuth angle β, but positively correlated with the elevation angle α and the measurement noise intensity σ.

V. SIMULATION

Computer simulations are presented in this section with three sets of examples. The first evaluates the influence of bias on localization performance to show the necessary of bias compensation. The second examines the bias behaviors to verify the theoretical analysis of bias estimate in section IV. The last one exhibits the bias compensation performance of the proposed method, by comparing it with the ML cost function method [22]. The satellite orbits around the earth with a orbital altitude $h = 700$ km, and the target altitude $h_0 = 0$ km. The yaw, pitch, and roll angles of the satellite are zero for ease of illustration, so that the coordinate transformation matrix $\boldsymbol{M} = \boldsymbol{I}_3$. The covariance matrix $\boldsymbol{Q} = \sigma^2\boldsymbol{I}_2$, where σ is the noise intensity of angle measurements.

We introduce the ratio of bias to CRLB (RB2C) as criterion to examine the effect of bias on localization accuracy,

$$\boldsymbol{RB2C}\left(\boldsymbol{x}_T^0\right) = \frac{\sqrt{\mathrm{tr}\left(\boldsymbol{CRLB}(\boldsymbol{x}_T^0)\right)}}{\left\|\boldsymbol{b}_{\boldsymbol{x}_T^0}\right\|}, \tag{43}$$

where tr(∗) denotes the trace of a matrix. The constrained CRLB of geolocation error $\boldsymbol{CRLB}(\boldsymbol{x}_T^0)$ is derived in Appendix. Apparently, the larger the $\boldsymbol{RB2C}\left(\boldsymbol{x}_T^0\right)$, the greater the influence of bias on localization accuracy.

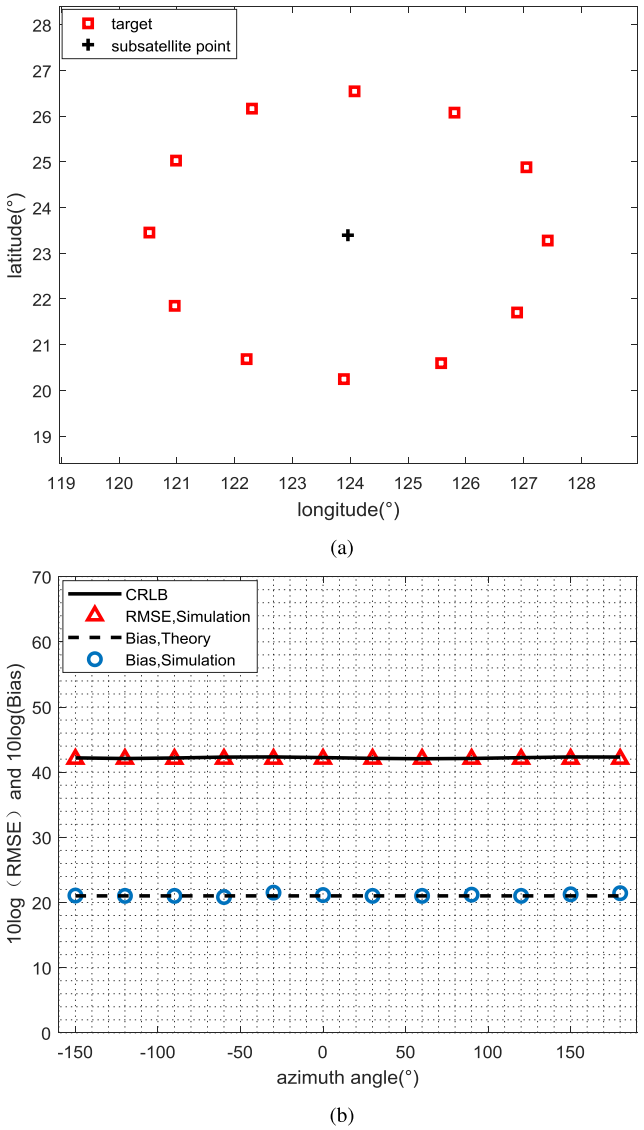

FIGURE 5. CRLB, RMSE, Theoretical and Simulation Bias versus azimuth angle. (a) Deployment. (b) Simulation Result.

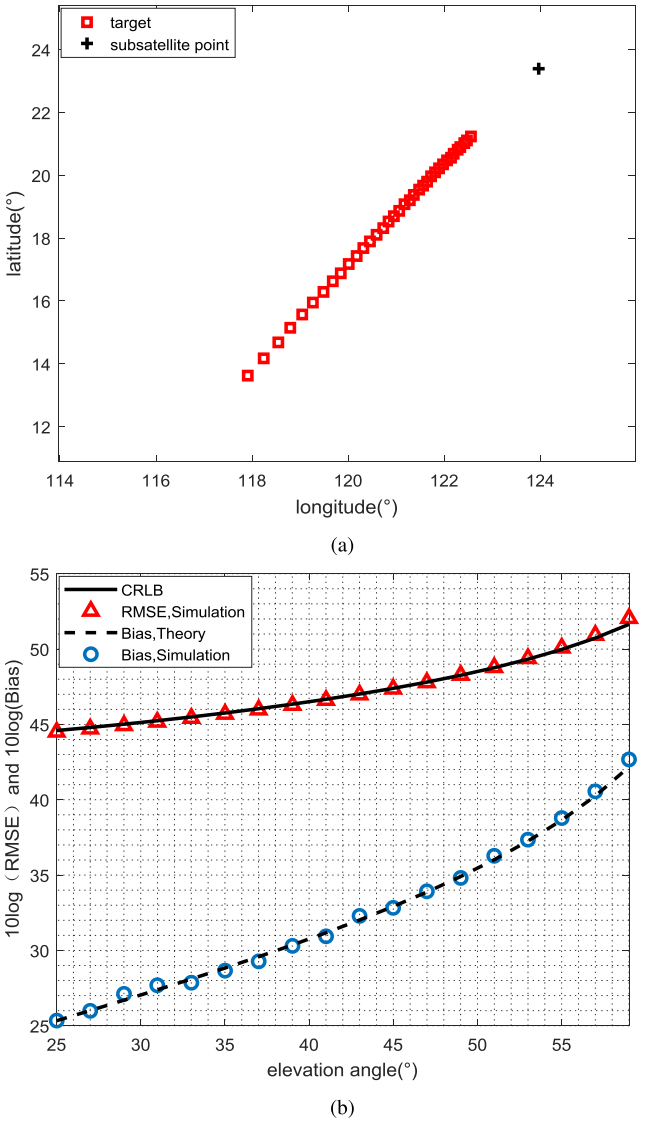

FIGURE 6. CRLB, RMSE, Theoretical and Simulation Bias versus elevation angle. (a) Deployment. (b) Simulation Result.

For each given simulation, the bias and RMSE (root mean square error) of the target position estimate are computed over $N = 100000$ ensemble runs, which are defined as follows.

$$\boldsymbol{Bias} = \left\| \frac{1}{N} \sum_{i=1}^{N} \left(\hat{\boldsymbol{x}}_T^i - \boldsymbol{x}_T^0 \right) \right\|, \tag{44}$$

$$\boldsymbol{RMSE} = \sqrt{\frac{1}{N} \sum_{i=1}^{N} \left\| \hat{\boldsymbol{x}}_T^i - \boldsymbol{x}_T^0 \right\|^2}, \tag{45}$$

where $\hat{\boldsymbol{x}}_T^i$ is the target position estimate at ensemble i.

A. RB2C ANALYSIS

Fig. 4 depicts the RB2C in different elevation angles and noise levels. The longitude and latitude of the subsatellite point is (123.96°, 23.39°) and the azimuth angle β^0 is fixed at 30°. The elevation angle α^0 varies from 20° to 60°, and the noise intensity σ is equal to 1°, 3°, 5°, 7° respectively.

It can be seen from Fig. 4 that the RB2C is positively correlated with the elevation angle and noise level. Without the loss of generality, we say a bias is not negligible when the RB2C is greater than 0.1. When the noise intensity $\sigma = 1°$, the RB2C is less than 0.1 for all elevation angles. When the noise intensity $\sigma = 7°$, the RB2C is greater than 0.1 when the elevation angle is greater than 40°. It can be seen that the bias cannot be ignored (RB2C > 0.1) under the circumstance that at high noise level and with large elevation angle (i.e., geolocation geometry is poor).

B. BIAS ANALYSIS

Fig. 5 shows the simulation results as a function of the azimuth angle. Therein, Fig. 5a is the geolocation scenario. There are 12 targets uniformly distributed around the

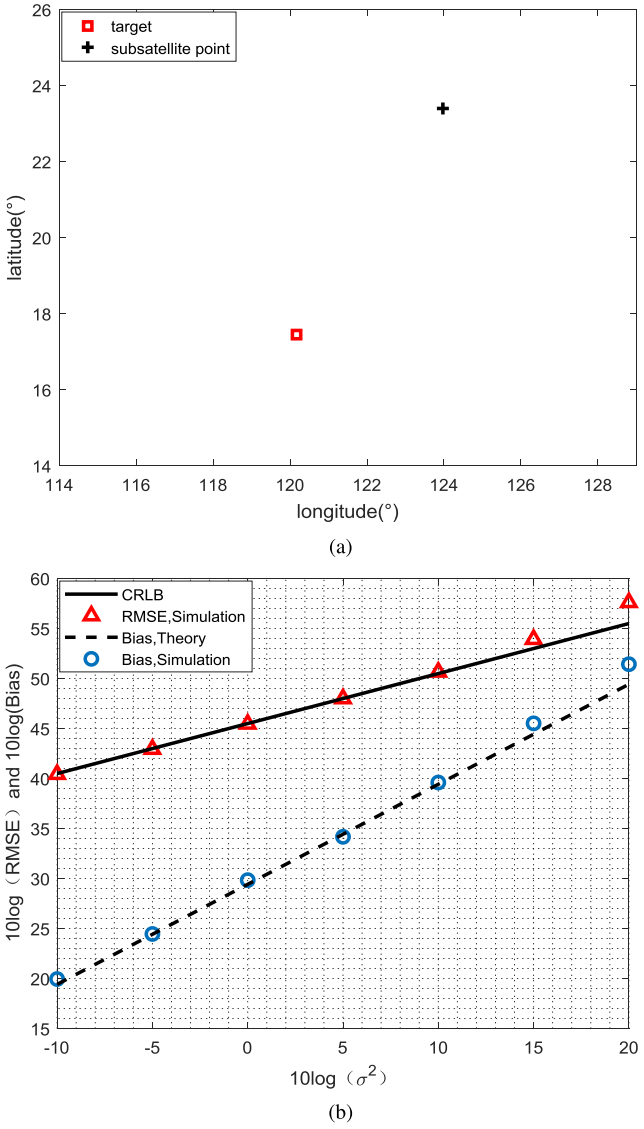

FIGURE 7. CRLB, RMSE, Theoretical and Simulation Bias versus measurements error variance σ^2. (a) Deployment. (b) Simulation Result.

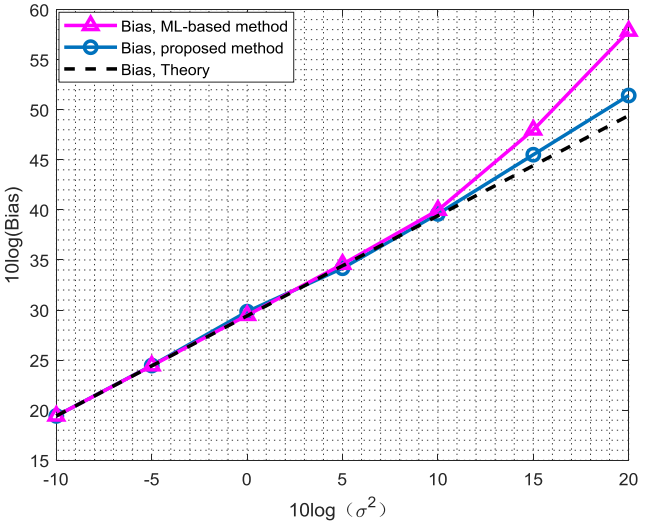

FIGURE 8. Comparison of bias estimate accuracy.

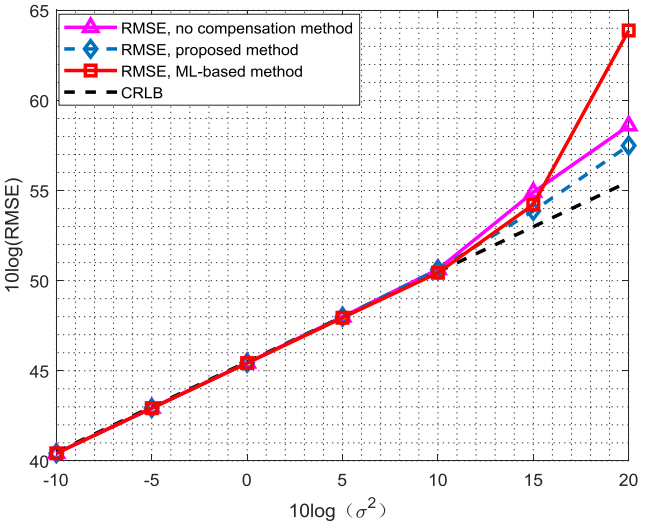

FIGURE 9. Comparison of bias compensation results in single measurement condition.

subsatellite point, the noise intensity σ and the elevation angle α^0 are fixed at 1° and 30° respectively.

It can be seen from Fig. 5b that the bias is independent of the azimuth angle, which is consistent with the theoretical analysis in (42). Besides, the CRLB and RMSE are also independent of the azimuth angle.

Fig. 6 shows the simulation results as a function of the elevation angle. The scenario is illustrated in Fig. 6a. The azimuth angle β^0 is fixed at 30° and the noise intensity $\sigma = 1°$. From Fig. 6b, we observe that the bias rises as the elevation angle increases. The results are consistent with the theoretical analysis in (42). Moreover, the bias rises faster than the CRLB and RMSE when the elevation angle increases.

Fig. 7 shows the results as a function of the angle measurements noise level. The real elevation angle and azimuth angle are fixed at $\alpha^0 = 50°$ and $\beta^0 = 30°$, as shown in Fig. 7a. It is found that the RMSE and bias increase with the noise level. The simulated and theoretical bias can match very well when the noise level is small, and the RMSE can reach the CRLB approximately. When the noise level increases (greater than 15 dB in Fig. 7), the simulated bias is bigger than the theoretical one. This is because that we ignore the expansion terms higher than second order, namely, the higher order series also should be considered when the noise level is too high.

Fig. 8 shows the bias estimate accuracy results as a function of the noise level. The accuracy of the proposed bias estimate method is compared with the maximum likelihood (ML)-based bias estimate method [22] using the same geometry in Fig. 7a. We found that both methods can estimate the bias accurately at a low noise level, but the proposed method outperforms the ML-based method in large noise intensity. The

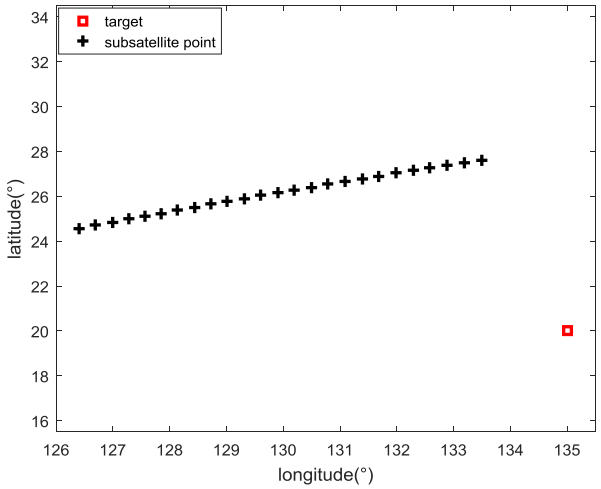

(a)

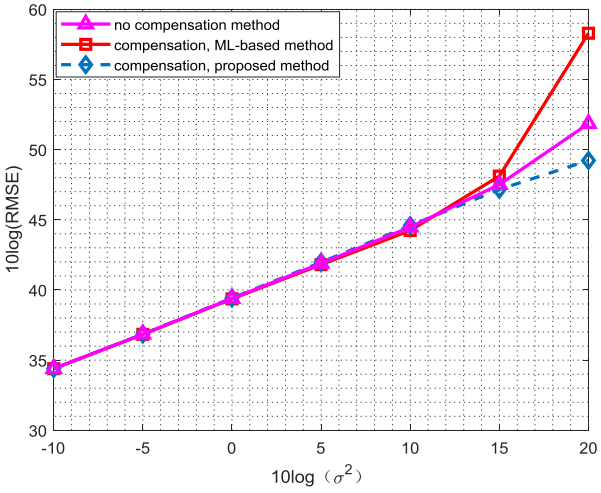

(b)

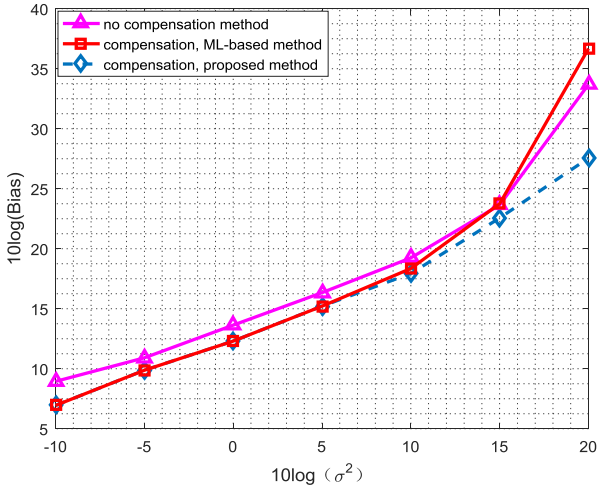

(c)

FIGURE 10. Comparison of bias compensation results in multiple measurements condition. (a) Deployment. (b) RMSE versus measurements error variance σ^2. (c) Bias versus measurements error variance σ^2.

simulation results verify the higher bias estimate accuracy of the proposed method over the ML-based method with the same order of Taylor-series expansion.

C. BIAS COMPENSATION

We provide two kinds of bias compensation results: single measurement and multiple measurements. They use the bias compensation methods in (31) and (32) respectively.

The geolocation performance of the proposed bias compensation method is compared with the CRLB, ML-based method [22], and no compensation method. The only difference between the proposed method and ML-based method is the estimated bias used for compensation. The no compensation method represents the original target location estimate results without bias compensation.

Fig. 9 shows the bias compensation results in single measurement condition. The scenario is described in Fig. 7a. It can be seen that all the RMSEs are close to the CRLB when the noise at a low noise (smaller than 10 dB). The proposed method can still improve the RMSE when the noise level is larger than 15 dB. However, the ML-based method cannot improve the RMSE at this time. On contrary, its RMSE is even bigger than that of the no compensation method. On account of that the ML-based method cannot estimate the bias accurately at high noise level (larger than 15 dB), so that the bias compensated RMSE is accordingly larger since it has subtracted a wrong bias.

Fig. 10 shows the bias compensation results in multiple measurements condition. The scenario is illustrated in Fig. 10a. The longitude and latitude of the target is (135°, 20°), and there are 25 subsatellite point with the elevation angle varying from 51.95° to 56.15°. This indicate that the geolocation geometry is very poor. The RMSE and bias results of all methods are shown in Fig. 10b and Fig. 10c respectively. It can be seen that the two bias compensation methods have almost the same performance when the noise level increase from −10 dB to 15 dB. Furthermore, the proposed method outperforms the ML-based method when the noise level is larger than 15 dB.

VI. CONCLUSION

This paper performs an in-depth analysis of the bias in geolocating a target on the surface of the Earth using AOA measurements. Bias is derived by Taylor-series expansion on the closed-form target location estimation, instead of the ML cost function in existing methods. This difference brings significant benefits from two aspects. First, the proposed bias estimate method has the property that the expectations of the odd-order Taylor-series expansion terms are equal to zero. In summary, we can achieve higher bias estimation accuracy with the same order of expansion compared with existing methods. Second, the relationship between bias and angle measurements can be shown more directly and clearly. We discover that the Euclidean norm of the bias is positively correlated with the elevation angle and the measurement noise intensity, but independent of the azimuth angle. Simulation results show that the proposed bias estimation and compensation method have better geolocation performance with high measurement noise level and poor geolocation geometry.

APPENDIX
CRLB OF GEOLOCATION ERROR

This appendix derives the CRLB of $\boldsymbol{x}_T^0$, denoted as $\boldsymbol{CRLB}(\boldsymbol{x}_T^0)$. As the target altitude h_0 is known, the CRLB of $\boldsymbol{x}_T^0$ would be an equality-constrained one. To simplify the derivation, we follow the re-parameterization approach [26] and establish $\boldsymbol{CRLB}(\boldsymbol{x}_T^0)$ via relating it to the CRLB of $\Phi^0 = \begin{bmatrix}\phi & \varphi\end{bmatrix}^{\mathrm{T}}$, where ϕ and φ are the target geodetic latitude and longitude. Specifically, we have [13]

$$\boldsymbol{CRLB}(\boldsymbol{x}_T^0) = \left(\frac{\partial \boldsymbol{x}_T^0}{\partial \Phi^0}\right) \boldsymbol{CRLB}(\Phi^0) \left(\frac{\partial \boldsymbol{x}_T^0}{\partial \Phi^0}\right)^{\mathrm{T}}, \quad (46)$$

Under the spherical Earth model, $\boldsymbol{x}_T^0$ is related to the target geodetic latitude and longitude via [2]

$$x_T^0 = (R + h_0)\cos(\phi)\cos(\varphi), \quad (47a)$$
$$y_T^0 = (R + h_0)\cos(\phi)\sin(\varphi), \quad (47b)$$
$$z_T^0 = (R + h_0)\sin(\phi). \quad (47c)$$

Thus, the partial derivatives $\dfrac{\partial \boldsymbol{x}_T^0}{\partial \Phi^0}$ is equal to

$$\frac{\partial \boldsymbol{x}_T^0}{\partial \Phi^0} = (R + h_0)\begin{bmatrix} -\sin(\phi)\cos(\varphi) & -\cos(\phi)\sin(\varphi) \\ -\sin(\phi)\sin(\varphi) & \cos(\phi)\cos(\varphi) \\ \cos(\phi) & 0 \end{bmatrix}. \quad (48)$$

It can be seen that under the independent Gaussian noise model for AOA measurements,

$$\boldsymbol{CRLB}(\Phi^0) = \left(\left(\frac{\partial \boldsymbol{x}_T^0}{\partial \Phi^0}\right)^{\mathrm{T}} \boldsymbol{F} \left(\frac{\partial \boldsymbol{x}_T^0}{\partial \Phi^0}\right)\right)^{-1}, \quad (49)$$

where $\boldsymbol{F}$ is the Fisher information matrix of the target position $\boldsymbol{x}_T^0$ [13], which can be calculated by differentiating (3) in matrix form,

$$\boldsymbol{F} = -\boldsymbol{E}\left[\frac{\partial^2 \ln p(\boldsymbol{m})}{\partial \boldsymbol{x}_T^2}\right] = \boldsymbol{J}^T \boldsymbol{Q}^{-1} \boldsymbol{J}, \quad (50)$$

where $\boldsymbol{J}$ is the Jacobian matrix, which can be calculated by

$$\boldsymbol{J} = \begin{bmatrix} \dfrac{\partial \alpha}{\partial x_T^0} & \dfrac{\partial \alpha}{\partial y_T^0} & \dfrac{\partial \alpha}{\partial z_T^0} \\ \dfrac{\partial \beta}{\partial x_T^0} & \dfrac{\partial \beta}{\partial y_T^0} & \dfrac{\partial \beta}{\partial z_T^0} \end{bmatrix}. \quad (51)$$

REFERENCES

[1] S. Hartzell, L. Burchett, R. Martin, C. Taylor, and A. Terzuoli, "Geolocation of fast-moving objects from satellite-based angle-of-arrival measurements," *IEEE J. Sel. Topics Appl. Earth Observ. Remote Sens.*, vol. 8, no. 7, pp. 3396–3403, Jul. 2015.

[2] F. Guo, Y. Fan, Y. Zhou, C. Xhou, and Q. Li, *Space Electronic Reconnaissance: Localization Theories and Methods*. Hoboken, NJ, USA: Wiley, 2014.

[3] Y. Wang and K. C. Ho, "An asymptotically efficient estimator in closed-form for 3-D AOA localization using a sensor network," *IEEE Trans. Wireless Commun.*, vol. 14, no. 12, pp. 6524–6535, Dec. 2015.

[4] D.-C. Chang and M.-W. Fang, "Bearing-only maneuvering mobile tracking with nonlinear filtering algorithms in wireless sensor networks," *IEEE Syst. J.*, vol. 8, no. 1, pp. 160–170, Mar. 2014.

[5] L. Badriasl and K. Dogancay, "Three-dimensional target motion analysis using azimuth/elevation angles," *IEEE Trans. Aerosp. Electron. Syst.*, vol. 50, no. 4, pp. 3178–3194, Oct. 2014.

[6] Z. Wang, J.-A. Luo, and X.-P. Zhang, "A novel location-penalized maximum likelihood estimator for bearing-only target localization," *IEEE Trans. Signal Process.*, vol. 60, no. 12, pp. 6166–6181, Dec. 2012.

[7] Z. Duan and Q. Zhou, "CRLB-weighted intersection method for target localization using AOA measurements," in *Proc. IEEE Int. Conf. Comput. Intell. Virtual Environ. Meas. Syst. Appl. (CIVEMSA)*, Jun. 2015, pp. 1–6.

[8] Z.-M. Liu, C. Zhang, and P. S. Yu, "Direction-of-arrival estimation based on deep neural networks with robustness to array imperfections," *IEEE Trans. Antennas Propag.*, vol. 66, no. 12, pp. 7315–7327, Dec. 2018.

[9] Z. Yang, L. Xie, and C. Zhang, "Off-grid direction of arrival estimation using sparse Bayesian inference," *IEEE Trans. Signal Process.*, vol. 61, no. 1, pp. 38–43, Jan. 2013.

[10] P. Xu, B. Yan, and S. Hu, "Angle of arrival (AOA)-based cross-localization algorithm using orientation angle for improved target estimation in far-field environments," *Int. J. Simul.-Syst., Sci. Technol.*, vol. 17, no. 25, pp. 20.1–20.8, 2016.

[11] Y. Wang and Z. Duan, "PLS initialized sequential estimator for target localization using AOA measurements," in *Proc. IEEE Int. Conf. Comput. Intell. Virtual Environ. Meas. Syst. Appl. (CIVEMSA)*, Jun. 2015, pp. 1–6.

[12] M. Soltanian, A. M. Pezeshk, A. Mahdavi, and M. Dallali, "A new iterative position finding algorithm based on taylor series expansion," in *Proc. 19th Iranian Conf. Elect. Eng.*, May 2011, pp. 1–4.

[13] S. M. Kay, *Fundamentals of Statistical Signal Processing, Volume I: Estimation Theory*. Upper Saddle River, NJ, USA: Prentice-Hall, 1993.

[14] M. Longbin, S. Xiaoquan, Z. Yiyu, S. Z. Kang, and Y. Bar-Shalom, "Unbiased converted measurements for tracking," *IEEE Trans. Aerosp. Electron. Syst.*, vol. 34, no. 3, pp. 1023–1027, Jul. 1998.

[15] L. Rui and K. C. Ho, "Bias analysis of source localization using the maximum likelihood estimator," in *Proc. IEEE Int. Conf. Acoust., Speech Signal Process. (ICASSP)*, Mar. 2012, pp. 2605–2608.

[16] A. L. Yang, B. F. Guo, C. L. Yang, D. Z. Min, and E. W. Jiang, "Bias analysis of an algebraic solution for tdoa localization with sensor location errors," in *Proc. 23rd Eur. Signal Process. Conf. (EUSIPCO)*, Sep. 2015, pp. 190–194.

[17] N. Adib, "Design, analysis, and optimization of bearings-only geolocation algorithms," Ph.D. dissertation, Lyle School Eng., Southern Methodist Univ., Dallas, TX, USA, May 2016.

[18] W. H. FOY, "Position-location solutions by Taylor-series estimation," *IEEE Trans. Aerosp. Electron. Syst.*, vol. AES-12, no. 2, pp. 187–194, Mar. 1976.

[19] K. Dogancay and D. A. Gray, "Bias compensation for least-squares multipulse TDOA localization algorithms," in *Proc. Int. Conf. Intell. Sensors, Sensor Netw. Inf. Process.*, Dec. 2005, pp. 51–56.

[20] K. Dogancay, "Bias compensation for the bearings-only pseudolinear target track estimator," *IEEE Trans. Signal Process.*, vol. 54, no. 1, pp. 59–68, Jan. 2006.

[21] M. Gavish and A. J. Weiss, "Performance analysis of bearing-only target location algorithms," *IEEE Trans. Aerosp. Electron. Syst.*, vol. 28, no. 3, pp. 817–828, Jul. 1992.

[22] L. Rui and K. C. Ho, "Bias analysis of maximum likelihood target location estimator," *IEEE Trans. Aerosp. Electron. Syst.*, vol. 50, no. 4, pp. 2679–2693, Oct. 2014.

[23] P. D. Groves, *Principles of GNSS, Inertial, and Multisensor Integrated Navigation Systems*. 2nd ed. Boston, MA, USA: Artech House, 2013.

[24] K. C. Ho and Y. T. Chan, "Geolocation of a known altitude object from TDOA and FDOA measurements," *IEEE Trans. Aerosp. Electron. Syst.*, vol. 33, no. 3, pp. 770–783, Jul. 1997.

[25] K. S. Marvin, *Probability Distributions Involving Gaussian Random Variables*. New York, NY, USA: Springer, 2006.

[26] T. J. Moore, R. J. Kozick, and B. M. Sadler, "The constrained Cramér-Rao bound from the perspective of fitting a model," *IEEE Signal Process. Lett.*, vol. 14, no. 8, pp. 564–567, Aug. 2007.

CHAOXIN HE received the B.S. degree in electronic engineering from the Beijing Institute of Technology Beijing, in 2012. He is currently pursuing the Ph.D. degree with the National University of Defense Technology (NUDT), Changsha, Hunan, China. His current research interests include passive source localization and radar signal processing.

MIN ZHANG received the Ph.D. degree in information and communication engineering from the School of Electronic Science and Engineering (ESE), National University of Defense Technology (NUDT), Changsha, Hunan, China, in 2014. His research interests include passive source localization and radar signal processing.

FUCHENG GUO received the Ph.D. degree in information and communication engineering from the School of Electronic Science and Engineering (ESE), National University of Defense Technology (NUDT), Changsha, Hunan, China, in 2002.

He is currently a Professor with the School of ESE, NUDT. His research interests include source localization and radar/communication signal processing.